



## Mechanism of inhibition of some imidazoline derivatives on iron surface using computational chemistry approach

K.J. Uwakwe <sup>1\*</sup>, A.I. Obike <sup>1,2</sup>

<sup>1</sup>Corrosion and Electrochemistry Research Group, Department of Pure and Applied Chemistry, University of Calabar, Calabar, Nigeria

<sup>2</sup> Department of Pure and Industrial Chemistry, Abia State University, Uturu, Abia State, Nigeria

Received 24 Nov 2017,  
Revised 08 Apr 2018,  
Accepted 01 May 2018

### Keywords

- ✓ Adsorption
- ✓ Imidazoline Derivatives
- ✓ Corrosion inhibition
- ✓ Iron
- ✓ Computational Chemistry

[kelechibenard@gmail.com](mailto:kelechibenard@gmail.com)

Phone: +234 809 232 6400

### Abstract

The adsorption/corrosion inhibitive potential of three (3) newly synthesized imidazoline derivatives namely (Z)-2-(2-(heptadec-8-en-1-yl)-4,5-dihydro-1H-imidazol-1-yl) ethan-1-amine (HDED), 2-(2-((10Z,13Z)-nonadeca-10,13-dien-1-yl)-4,5-dihydro-1H-imidazol-1-yl) ethan-1-amine (NDDE) and 2-(2-heptadecyl-4,5-dihydro-1H-imidazol-1-yl) ethan-1-amine (HDDE) on iron was determined by Quantum chemical calculations and Molecular dynamic simulation methods using the Material studio software package. The results obtained from the quantum chemical calculations (semi empirical and density functional theory (DFT) calculations) revealed that the active sites for adsorption on these molecules are the N=C-N region present in the heterocyclic ring for all the molecules studied, and the double bonded carbon atoms present in the alkyl hydrophobic tail of the molecules for HDED and NDDE respectively. The results obtained from the molecular dynamic simulation revealed that the molecules are attached unto the iron surface in a perpendicular manner using the heterocyclic ring. Both the quantum chemical calculations and the molecular dynamic simulation gives the adsorption/corrosion inhibitive potential of these molecules in decreasing order as NDDE > HDED > HDDE. The molecules are said to be physically adsorb on the iron surface.

## 1. Introduction

Corrosion causes the destruction or deterioration of metals by chemical means in environments to which they are exposed and results in enormous economic losses [1]. Among the various methods of mitigating corrosion, the use of corrosion inhibitor is one of the best and most economical methods. Thus, there is a need in studying the inhibition efficiency of different chemical compounds. Corrosion inhibitors are chemical compounds, whose presence in small quantities can retard corrosion of metal in aggressive environments. They are mainly organic compounds which slows down the corrosion process of a metal through the mechanism of adsorption and act by forming a barrier to oxygen and moisture, by complexing with metal ions or by removing corrodents from the environment [2], which is influenced by factors such as steric effect, electronic structure, aromaticity, electron density at the donor atoms and p-orbital character of the donating electrons [3]. Generally, the inhibiting mechanism can be explained by the formation of a physical and/or chemically adsorbed film on the metal surface [4]. Amines and their derivatives are well known as corrosion inhibitors for iron and its alloys, their relatively high-water solubility is an advantage for their use as inhibitors [5]. Imidazoline is a typical amine-nitrogen compound which is heterocyclic in nature. Heterocyclic organic compounds consisting of a  $\pi$ -system or heteroatoms such as N, S, or O are said to be good corrosion inhibitors [6]. The lone electrons present in the hetero atoms, size, suitable functional groups, multiple bonds and the planarity of a molecule are important features that determine the adsorption of molecules on a metallic surface [7]. The adsorbed molecules can affect the corrosion reaction, either by the blocking effect of the adsorbed molecules on the metal surface or by the effect attributed to the change in the activation barriers of the anodic and cathodic reactions of the corrosion process. [8]. A molecule with a good adsorption ability will not be easily desorbed from the surface of a material either by a higher temperature or by other external factors. Therefore, we can say that the better the adsorption ability of a molecule, the better is its corrosion inhibition efficiency.

Computational studies which includes molecular dynamic simulation and quantum chemical calculations have shown to be very effective in providing information such as the most stable molecular conformation and adsorption sites for a broad range of materials [9-12]. This information can help to gain further insight into the corrosion system, such as the most likely point of attack for corrosion on a surface, the most stable site for adsorption on a molecule, adsorption density of a molecule and the binding energy of the adsorbed layer. Quantum chemistry methods have proved to be a very useful and powerful tool for determining the adsorption and inhibitive potential of different compounds, due to the fact that there is a strong relationship between the corrosion inhibition efficiency and the adsorption ability of most compounds with several quantum chemical parameters such as the works reported on Phthalazine derivatives [11], Triazole derivatives [13], Pyrazine derivatives [10] and Thiophene derivatives [14] just to name a few. Furthermore, molecular dynamic simulations have been used to study the structural changes, energetics and interactions between several compounds on a metal surface [15, 16]. In this study two (2) imidazoline derivatives consisting mainly of the head (heterocyclic ring), the anchor or pendant (the substituent attached to the heterocyclic ring) and the tail (the long alkyl hydrophobic tail) [17] and one (1) imidazoline derivative consisting of just the head and the tail were investigated to determine their adsorption/corrosion inhibitive potential on iron, this will help in predicting the experimental outcomes before they are done so that we can be better prepared to make observation and to perform more intelligent experiments. The names, abbreviations, chemical formulas, structures and molecular weights of these newly synthesized imidazoline derivatives are shown in Table 1.

**Table 1:** Names, abbreviations, chemical formulas, structures and molecular weights of the newly synthesized imidazoline derivatives.

Name	Abbreviation	Chemical Formula	Schematic Structure of the molecule	Molecular Weight(g/mol)
(Z)-2-(2-(heptadec-8-en-1-yl)-4,5-dihydro-1H-imidazol-1-yl)ethan-1-amine	HDED	C <sub>22</sub> H <sub>43</sub> N <sub>3</sub>		349.61
2-(2-((10Z,13Z)-nonadeca-10,13-dien-1-yl)-4,5-dihydro-1H-imidazol-1-yl)ethan-1-amine	NDDE	C <sub>24</sub> H <sub>45</sub> N <sub>3</sub>		375.65
2-(2-heptadecyl-4,5-dihydro-1H-imidazol-1-yl)ethan-1-amine	HDDE	C <sub>20</sub> H <sub>40</sub> N <sub>2</sub>		308.56

## 2. Computational Details

### 2.1. Computational details for quantum chemical calculations

The quantum chemical calculations were done using the Dmol<sup>3</sup> and the Vamp module present in the Material studio software package [18]. Using the Vamp module (which is a semi empirical molecular orbital package for organic and inorganic system), theoretical calculations were carried out at the Restricted Hartree-Fock level (RHF), using the Hamiltonian parametric method 3 (PM3) which is based on the neglect of diatomic differential overlap (NDDO) approximation. Using the Dmol<sup>3</sup> module, theoretical calculations were performed using the Density functional theory (DFT) method in combination with the BLYP (from the name Becke for the exchange part and Lee, Yang and Parr for the correlation part) functional method via the Double numeric with polarization (DNP) basic set, which is the best basic set in Dmol<sup>3</sup> module [19]. DFT methods have been found to be accurate in providing information on frontier molecular orbitals, chemical reactivity and selectivity in terms of energy and global parameters such as energy of the highest occupied molecular orbital ( $E_{HOMO}$ ), energy of the lowest unoccupied molecular orbital ( $E_{LUMO}$ ), ionization potential ( $IE$ ), electronegativity ( $\chi$ ), electron affinity ( $EA$ ), global hardness ( $\eta$ ), global softness ( $\sigma$ ) etc. From Koopmans theorem, the ionization potential ( $IE$ ) and the electron affinity ( $EA$ ) of a molecule are given as [20]:

$$IE = -E_{HOMO} \quad (1)$$

$$EA = -E_{LUMO} \quad (2)$$

According to Pearson, the values of the electronegativity and the global hardness are calculated as [21]:

$$\chi = IE+EA/2 \quad (3)$$

$$\eta = IE-EA/2 \quad (4)$$

The global softness is the reciprocal of the global hardness as shown in equation 5:

$$\sigma = 1/\eta \quad (5)$$

when two systems, iron and a molecule are in contact, electrons will flow from lower  $\chi$ (molecule) to higher  $\chi$ (iron), until the chemical potential becomes equal. The number of electron transferred  $\Delta N$  can be calculated using this expression [22]:

$$\Delta N = \chi_{Fe} - \chi_{mole} / [2(\eta_{Fe} + \eta_{mole})] \quad (6)$$

where  $\chi_{Fe}$  and  $\chi_{mole}$  is the electronegativity of iron and the molecule respectively, while  $\eta_{Fe}$  and  $\eta_{mole}$  is the global hardness of iron and the molecule respectively. Equation 6 can also be written as

$$\Delta N = \phi_{Fe} - \chi_{mole} / 2\eta_{mole} \quad (7)$$

where  $\phi_{Fe}$  is the work function of the Fe (001) surface whose theoretical value is given as 4.08 eV [23] and  $\eta_{Fe} = 0$  is used assuming that for a metallic bulk  $IE = EA$  [24] because they are softer than the neutral metallic atoms. We chose the Fe (001) surface because atoms exchange with substrate surface atoms occur frequently on the Fe (001) surface [25]. Parr *et al.* [26] also introduced an electrophilicity index ( $\omega$ ) which is given as:

$$\omega = \chi^2/2\eta \quad (8)$$

This is the electrophilic power of a molecule. i.e. the higher the value of  $\omega$ , the higher the ability of the molecule to accept electrons. This reactive index measures the stabilization in energy when a system gain an additional electronic charge from the environment.

The local reactivities of the molecules were studied using the Fukui indices [27]. The Fukui indices are measures of chemical reactivity, as well as an indicative of the reactive regions for electrophilic and nucleophilic attacks on the molecules. The regions of a molecule where the Fukui indices values are high is chemically softer than the regions where the Fukui indices values are low. The change in electron density is the electrophilic  $f_k^-$  and nucleophilic  $f_k^+$  Fukui functions, which can be calculated using the finite difference approximation as follows [28]:

$$f_k^- = q_N - q_{N-1} \quad (9)$$

$$f_k^+ = q_{N+1} - q_N \quad (10)$$

where  $q_N$ ,  $q_{N+1}$  and  $q_{N-1}$  are the electronic population of the atom  $k$  in neutral, anionic and cationic system. The  $N$  stands for the number of electrons in the molecule,  $N+1$  stands for an anion with an electron added to the LUMO of the neutral molecule, while  $N-1$  stands for the cation with an electron remove from the HOMO of the neutral molecule.

## 2.2. Computational details for molecular dynamic simulation

Adsorption behaviour of a molecule is very important in understanding its corrosion behaviour on a metal surface. Molecular dynamic simulation can reasonably predict the most favourable configuration of the adsorbed molecule on a metal surface [29]. The molecular dynamic simulation was done in a simulation box with dimensions (20.1 Å x 8.6 Å x 34.4 Å), and with a periodic boundary conditions to model a representative part of the interface devoid of any arbitrary effects. The box consists of an iron slab and a vacuum layer of height 28.1 Å. The Fe crystal was cleaved along the (0 0 1) plane with the topmost layer released and the internal layer fixed. The iron substrate with (0 0 1) plane was first optimized to the minimum energy. Then the molecules are placed near to the Fe (0 0 1) surface plane in each of the simulation box. The behaviour of the molecules on the Fe (0 0 1) surface was then simulated using the Forcite module (which is an advanced classical molecular mechanical tool that allows fast energy calculations and reliable geometry optimization of molecules and periodic system) to predict the most favourable configurations of the adsorbed molecules on the iron surface. The simulations were done at the temperature of 333 K in a vacuum/gas phase environment, using a time step of 0.1 femto second and a simulation time of 5 ps. A simulation time of 5ps was used to reduce the time spent on each run. The number of particles and the volume of each system in the ensemble are constant, and the ensemble has a well-defined temperature (NVT Ensemble). The force field Consistent Valence Force Field (CVFF) was used for the simulation operations. It is mainly used for the study of structures and binding energy, though it can also accurately predict vibrational frequencies and conformation energy. The interaction energies for the three (3) molecules were calculated using equation 11 [9]:

$$E_{interaction} = E_{complex} - E_{Fe} - E_{molecule} \quad (11)$$

$E$  in equation 11 stands for energy, therefore,  $E_{interaction}$  is the interaction energy,  $E_{complex}$  is the total energy of the Fe crystal together with the adsorbed molecule,  $E_{Fe}$  is the total energy of the Fe crystal and  $E_{molecule}$  is the total energy of the adsorbed molecule. The binding energy is the negative energy of the interaction energy as expressed in equation 12

$$E_{binding} = - E_{interaction} \quad (12)$$

Before these calculations were done, the molecules were sketched, the hydrogens were adjusted, and the molecules were cleaned using sketch tool available in the material visualizer. The colour codes for the atoms in the molecules studied are gray for carbon, blue for nitrogen and white for hydrogen. And the atoms have been numbered (Figure 1), for an in depth understanding of the role played by each of the atoms present in the molecules.

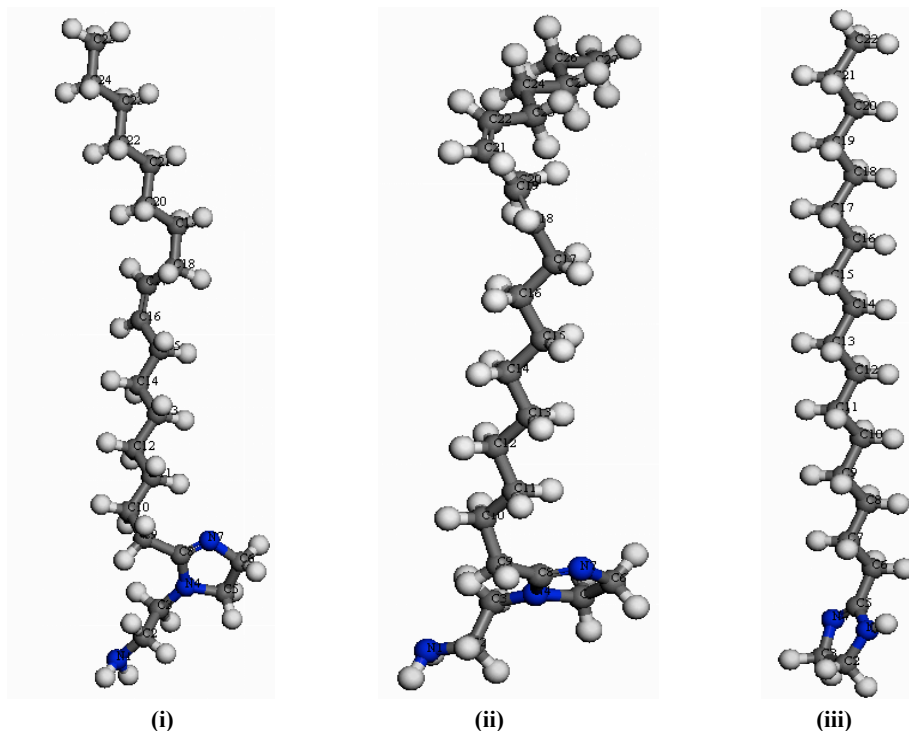
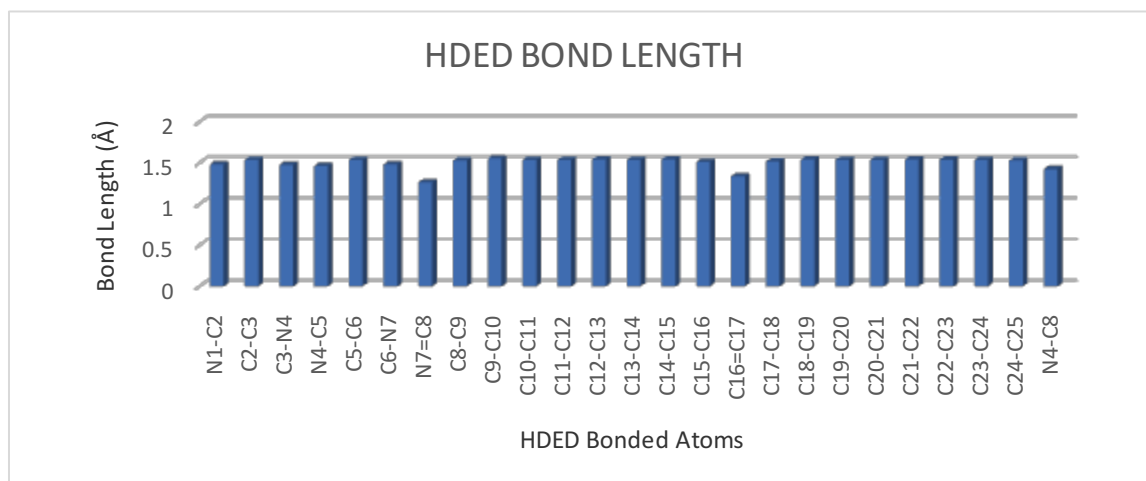


**Figure 1:** Geometry optimized structures with the atoms numbered for (i) HDED (ii) NDDE and (iii) HDDE molecules

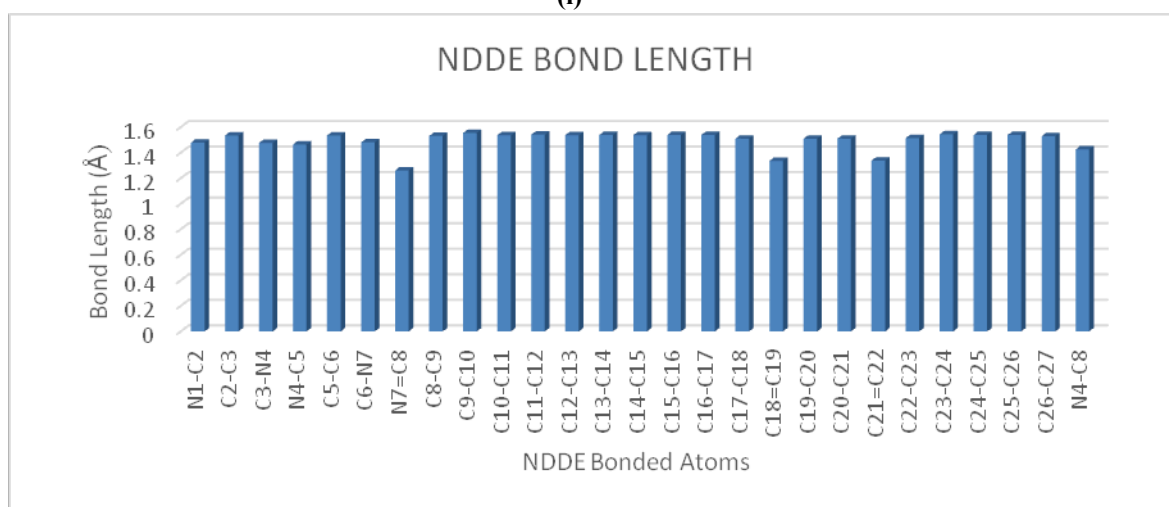
### 3. Results and Discussion

#### 3.1. Bond length, bond order and natural atomic charge

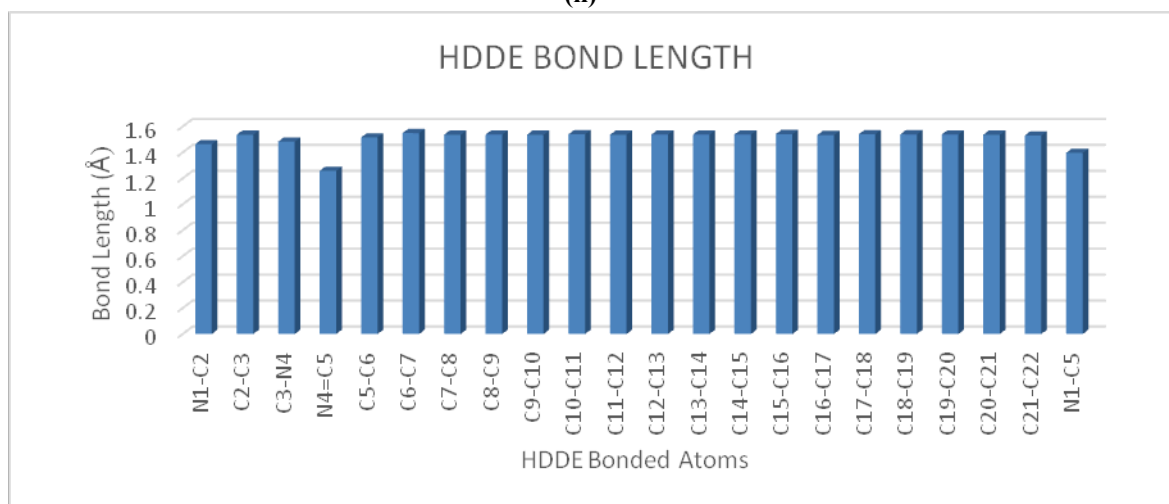
The bond length or bond distance is the average distance between two bonded atoms in a molecule. The bond lengths in Armstrong unit ( $\text{\AA}$ ) for HDED, NDDE and HDDE is shown in Figure 2. It is observed that the N7=C8 and C16=C17 bonds in HDED, the N7=C8, C18=C19 and C21=C22 bonds in NDDE, and the N4=C5 bond in HDDE are shorter compared to the others. Shorter bond length requires high dissociation energies to break the bond. This means that the closer the nuclei of the bonding atoms, the more energy is needed to separate the atoms due to large force of attraction between the atoms and hence the higher is the chemical reactivity of the bond which can also lead to higher adsorption/corrosion inhibitive effect [12]. From classical chemical theory, all chemical interactions can be by orbital interactions or by electrostatic interaction. The presence of electric charge in the molecule is the propelling force of an electrostatic interaction. Local electric charges have been proven to be vital in several chemical reactions as well as physiochemical characteristics of compounds [9]. Table 2 shows the natural atomic charges in coulombs (C) for the three (3) molecules studied. The N1, N4, N7 and C25 atoms in HDED, the N1, N4, N7 and C27 atoms in NDDE and the N1, N4 and C22 atoms in HDDE show a much lower charge than the other atoms, thereby making them possible sites for adsorption on the molecules. The C8 atoms in HDED and NDDE and the C5 atom in HDDE which are between two N atoms is very much electron deficient and are highly positively charged. This may be due to the highly electronegative nature of the two N atoms. This deficiency of electron in the C8 atoms in HDED and NDDE and the C5 atom in HDDE also makes them possible sites for adsorption on the molecule. The hydrogen atoms in the three (3) molecules studied are all positively charged.



(i)



(ii)



(iii)

**Figure 2:** Bond length and bond order analysis for (i) HDED (ii) NDDE and (iii) HDDE molecules

### 3.2. Energy and global parameters

The calculated energy and global parameters includes the energy of highest occupied molecular orbital ( $E_{HOMO}$ ), energy of lowest unoccupied molecular orbital ( $E_{LUMO}$ ), energy gap ( $\Delta E$ ), total energy ( $TE$ ), dipole moment ( $\mu$ ), energy of deformation ( $D$ ), van der Waal accessible area ( $A$ ), electronegativity ( $\chi$ ), electron affinity ( $EA$ ), ionization potential ( $IE$ ), global hardness ( $\eta$ ), global softness ( $\sigma$ ), fraction of electrons transferred ( $\Delta N$ ), and the electrophilicity index ( $\omega$ ) are shown in Table 3.

**Table 2:** Natural atomic charge for HDED, NDDE and HDDE atoms

HDED		NDDE		HDDE	
Atom	Charge	Atom	Charge	Atom	Charge
N1	-0.639	N1	-0.639	N1	-0.486
C2	-0.164	C2	-0.164	C2	-0.131
C3	-0.097	C3	-0.098	C3	-0.082
N4	-0.358	N4	-0.359	N4	-0.314
C5	-0.109	C5	-0.110	C5	0.307
C6	-0.097	C6	-0.097	C6	-0.241
N7	-0.341	N7	-0.337	C7	-0.281
C8	0.316	C8	0.319	C8	-0.286
C9	-0.237	C9	-0.234	C9	-0.276
C10	-0.289	C10	-0.288	C10	-0.277
C11	-0.258	C11	-0.256	C11	-0.277
C12	-0.289	C12	-0.289	C12	-0.278
C13	-0.288	C13	-0.276	C13	-0.277
C14	-0.276	C14	-0.279	C14	-0.278
C15	-0.246	C15	-0.285	C15	-0.277
C16	-0.129	C16	-0.250	C16	-0.277
C17	-0.107	C17	-0.243	C17	-0.277
C18	-0.240	C18	-0.135	C18	-0.279
C19	-0.273	C19	-0.092	C19	-0.279
C20	-0.261	C20	-0.195	C20	-0.264
C21	-0.281	C21	-0.131	C21	-0.285
C22	-0.281	C22	-0.111	C22	-0.442
C23	-0.264	C23	-0.242		
C24	-0.286	C24	-0.287		
C25	-0.441	C25	-0.268		
		C26	-0.285		
		C27	-0.440		

According to the frontier molecular orbital theory, the formation of a transition state is due to an interaction between frontier orbitals (HOMO and LUMO) of reacting species. HOMO is often associated with the electron donating ability of a molecule, whereas LUMO indicates its ability to accept electrons. The widely-accepted concept about a molecule adsorption mechanism is that: the higher the HOMO energy, the greater the tendency of offering electrons to the metal surface atoms, and the higher the adsorption/corrosion inhibitive effect. Similarly, the lower the LUMO energy, the greater the tendency of the molecules to accepting electrons from the metal surface atoms, and the better the adsorption/corrosion inhibitive effect [30]. From Table 3, NDDE shows the highest HOMO and the least LUMO energy, followed by HDED, while HDDE shows the least HOMO and the highest LUMO energy. The negative signs observed on the  $E_{HOMO}$  values shows that the adsorption is physisorption [31]. The energy gap ( $\Delta E = E_{LUMO} - E_{HOMO}$ ) is a very important parameter in determining the adsorption ability of a molecule due to the fact that it qualifies a molecule stability in chemical reactions. A decrease in the energy gap usually leads to easier polarization of the molecule. Smaller energy gap means better adsorption ability hence better inhibitive efficiency for the reason that lower excitation energy will be required to take away an electron from the last occupied orbital [32]. From Table 3, NDDE show a smaller energy gap than the rest of the molecules followed by HDED.

Apart from determining the adsorption/corrosion inhibitive ability of a molecule, the frontier molecular orbital (FMO) theory is also used to predict the adsorption centers of inhibitor molecules which are responsible for the interaction with a metal surface atom. These sites are shown in Figure 3,4 and 5, the HOMO orbital is mainly located on the heterocyclic ring and the pendent part of the molecules, but more on the heterocyclic ring part both for HDED and NDDE, for HDDE, the HOMO orbital is located on the heterocyclic ring part only.

**Table 3:** Energy and global parameters calculations for HDED, NDDE and HDDE

Energies and Global Parameters	HDED	NDDE	HDDE
$E_{HOMO}$ (eV)	-4.209	-4.194	-4.353
$E_{LUMO}$ (eV)	0.106	-0.008	0.530
$\Delta E$ (eV)	4.315	4.186	4.883
$TE$ (eV)	61	63	31
$IE$ (eV)	4.209	4.194	4.353
$EA$ (eV)	-0.106	0.008	-0.530
$\mu$ (Debye)	4.19	4.59	4.61
$D$ (eV)	1642	1700	1360
$\alpha$ ( $\text{\AA}^2$ )	526	560	475
$\chi$	2.05	2.10	1.91
$\eta$	2.16	2.09	2.44
$\sigma$	0.46	0.48	0.41
$\Delta N$	0.470	0.474	0.445
$\omega$	0.97	1.10	0.75

The LUMO orbital is mainly located in the double bonds between the carbon atoms C16=C17 for HDED and C18=C19 and C21=C22 for NDDE. The isosurface colour of the orbital plots shows the electron density difference, the blue regions show electron accumulation, while the yellow regions show electron loss. The total energy of the three (3) molecules are low, indicating that the molecules are in the geometry optimized state. Dipole moments as well as energy of deformability are parameters characterizing the interaction between molecules [9]. Dipole moment tells us about the charge separation in a molecule. The larger the difference in electronegativity of bonded atoms the larger the dipole moment [33]. Molecules with lower dipole moment has been reported to show good adsorption/corrosion inhibitive effect [34], also molecules with higher dipole moments have equally been shown to have good adsorption/corrosion inhibitive effect [35]. Therefore, the dipole moment is not a significant factor in concluding the expected trend in adsorption. Deformation energy on the other hand is the energy required to change the orientation of a molecule. The deformation energy can also be used to determine the stability of a molecule. NDDE show a higher deformation energy, meaning that a higher energy is needed to change the orientation of the molecule which signifies that the molecule is very stable. The van der Waal accessible surface or solvent accessible surface area is the surface area of a biomolecule that is accessible to a solvent. Table 3 shows the van der Waal accessible surface for HDED, NDDE and HDDE molecules respectively, and it is seen that NDDE has a larger surface area compared to HDED and HDDE. This may contribute to the high adsorption/corrosion inhibitive potential of NDDE compared to the other molecules, due to the fact that there is more accessible surface available on the molecule for adsorption to place [12], or we can say that this solvent accessible surface can act as a barrier between the iron and moisture present in the environment which is an agent of corrosion. The electronegativity of the three (3) molecules studied is lower than the work function of the Fe (001) surface which is 4.08 eV, this means that electrons can flow freely from the molecules to the iron surface until the chemical potential are the same.

Another important parameter which is used to measure the molecular stability as well as reactivity of a molecule is the global hardness and global softness. Global hardness fundamentally suggests the resistance towards the deformation or polarization of the electron cloud of the atoms, ions or molecules under small perturbation of chemical reaction. A hard molecule has a large energy gap and a soft molecule has a small energy gap [36]. Normally, the molecule with the least value of global hardness (hence the highest value of global softness) is expected to have the highest adsorption/corrosion inhibitive ability [37]. NDDE has the least value of global hardness and the highest value of global softness compared to HDED and HDDE. The fraction of electrons transferred from the molecules to the iron surface was calculated for HDED, NDDE and HDDE as listed in Table 3. According to Lukovits, if  $\Delta N < 3.6$ , the inhibition efficiency increased with increasing electron-donating ability by the molecule to the metal surface [37]. In this study, the values of  $\Delta N$  for HDED, NDDE and HDDE were less than 3.6, this shows that the increase in corrosion inhibitive ability was due solely to the electron donating ability of these molecules. We can say that the part of the molecules with high HOMO density will be oriented toward the iron surface. Higher fraction of electron transfer indicates better adsorption/corrosion inhibitive effect leading to better inhibition efficiency, and from Table 3, NDDE shows the highest number of electron transfer followed by HDED, this confirms the high adsorption/corrosion inhibitive

potential of NDDE established earlier by  $E_{HOMO}$ ,  $E_{LUMO}$ ,  $\Delta E$ ,  $\eta$  and  $\sigma$ . The adsorption/corrosion inhibitive ability of the molecules in decreasing order is given as NDDE > HDED > HDDE. The electrophilic power of NDDE is higher compared to the other molecules studied, that is the higher the ability of NDDE to accept electron from the iron surface which can also aid adsorption. But due to the fact that the fraction of electron transfer ( $\Delta N < 3.6$ ), the adsorption is said to be caused mainly by the donation of electrons by NDDE to the iron surface. So, a higher electrophilic power is not too relevant in this context. But it also proves the high adsorption/corrosion inhibitive potential of NDDE compared to the other molecules, because a good inhibitor should be able to donate and accept electrons freely when interacting with a surface.

### 3.3. Local reactivity

To establish the active sites of a molecule, three influencing and controlling factors: natural atomic charge, distribution of frontier molecular orbital and Fukui indices have to be considered [9]. Local reactivity is analyzed by means of the condensed Fukui function. Condensed Fukui functions allow us to distinguish each part of the molecule on the basis of its distinct chemical behaviour due to the different substituent functional groups. The nucleophilic and electrophilic attack is controlled by the maximum values of  $f_k^+$  and  $f_k^-$ . Electrophilic attack is synonymous to the function of the HOMO orbital, while the nucleophilic attack is synonymous to the function of the LUMO orbital, due to the fact that for a finite system such as a molecule, the parts of the molecule where electrons are accepted is the sites for nucleophilic attack; the parts of a molecule that donates electrons to a surface is the sites for electrophilic attack. This can be noticed in the frontier molecular orbital plots and the Fukui indices plots on the three molecules in Figure 3,4 and 5, but that doesn't mean that the Fukui indices sites can't be found elsewhere in the molecule where the HOMO and LUMO orbitals are not present. The calculated Fukui indices for electrophilic and nucleophilic attack for the three (3) selected molecules are tabulated in Table 4 (only C and N atoms are quoted), and their active sites are plotted on the molecules in Figures 3,4 and 5.

**Table 4:** Fukui negative ( $f_k^-$ ) and positive ( $f_k^+$ ) indices values for HDED, NDDE and HDDE atoms

HDED			NDDE			HDDE		
Atom	$f_k^-$	$f_k^+$	Atom	$f_k^-$	$f_k^+$	Atom	$f_k^-$	$f_k^+$
N1	0.010	-0.001	N1	0.009	-0.002	N1	0.179	0.030
C2	-0.018	-0.004	C2	-0.018	-0.002	C2	-0.050	-0.034
C3	-0.038	-0.012	C3	-0.039	-0.005	C3	-0.043	-0.043
N4	0.146	0.011	N4	0.148	0.004	N4	<b>0.196</b>	0.153
C5	-0.042	-0.009	C5	-0.042	-0.004	C5	0.028	<b>0.154</b>
C6	-0.038	-0.012	C6	-0.037	-0.005	C6	-0.018	-0.039
N7	<b>0.173</b>	0.068	N7	<b>0.172</b>	0.022	C7	-0.016	-0.039
C8	0.027	<b>0.090</b>	C8	0.028	0.032	C8	-0.010	-0.016
C9	-0.018	-0.012	C9	-0.018	-0.005	C9	-0.008	-0.012
C10	-0.012	-0.017	C10	-0.014	-0.007	C10	-0.006	-0.008
C11	-0.009	-0.009	C11	-0.009	-0.004	C11	-0.004	-0.005
C12	-0.006	-0.009	C12	-0.007	-0.004	C12	-0.003	-0.004
C13	-0.004	-0.011	C13	-0.004	-0.005	C13	-0.002	-0.003
C14	-0.004	-0.020	C14	-0.004	-0.006	C14	-0.002	-0.002
C15	-0.001	-0.038	C15	-0.003	-0.007	C15	-0.001	-0.002
C16	-0.008	0.069	C16	-0.002	-0.025	C16	-0.001	-0.001
C17	0.007	0.069	C17	-0.001	-0.028	C17	-0.001	-0.001
C18	-0.003	-0.040	C18	-0.004	0.074	C18	-0.001	-0.001
C19	-0.001	-0.016	C19	0.004	0.030	C19	-0.001	-0.001
C20	-0.001	-0.012	C20	0.000	-0.043	C20	-0.001	-0.001
C21	-0.001	-0.006	C21	-0.003	0.045	C21	-0.001	-0.001
C22	0.000	-0.004	C22	0.002	<b>0.080</b>	C22	-0.001	-0.001
C23	-0.001	-0.004	C23	0.000	-0.034			
C24	-0.001	-0.004	C24	0.000	-0.015			
C25	-0.001	-0.004	C25	0.000	-0.010			
			C26	-0.001	-0.008			
			C27	0.000	-0.007			

From Table 4, the sites for electrophilic attack on HDED and NDDE is the N4 and N7 atoms, with the N7 atoms having the maximum value of  $f_k^-$ , making it the major site for electrophilic attack on these molecules. The sites for nucleophilic attack for HDED is the N7, C8, C16 and C17 atoms, with the C8 atom having the maximum value of  $f_k^+$ , making it the major site for nucleophilic attack on the molecule. The sites for nucleophilic attack for NDDE is the N7, C8, C18, C19, C21 and C22 atoms, with the C22 atom having the maximum value of  $f_k^+$ , making it the major site for nucleophilic attack on the molecule. The sites for electrophilic attack in HDDE is the N1 and N4 atoms, with the N4 atom having the maximum value of  $f_k^-$ , making it the major site for electrophilic attack on the molecule. The sites for nucleophilic attack for HDDE is the N1, N4 and C5 atoms, with the C5 atom having the maximum value of  $f_k^+$ , making it the major site for nucleophilic attack on the molecule.

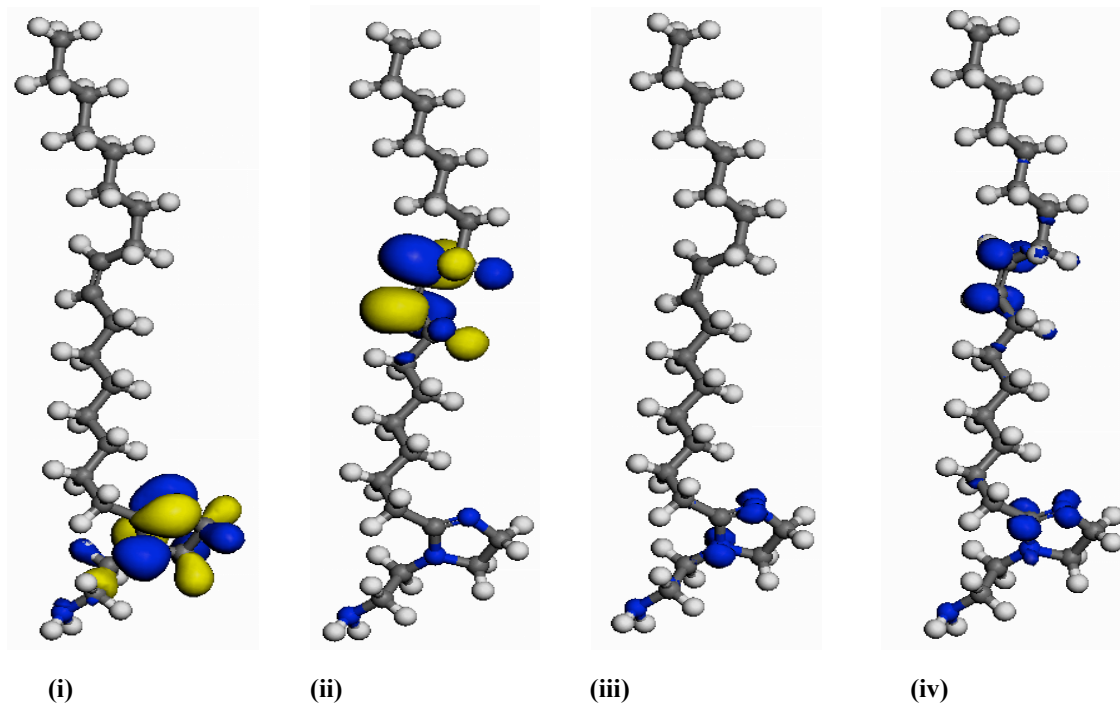


**Figure 3** (i) HOMO orbital plot (ii) LUMO orbital plot (iii) Plot for Fukui negative sites for electrophilic attack (iv) Plot for Fukui positive sites for Nucleophilic attack for HDED molecule.

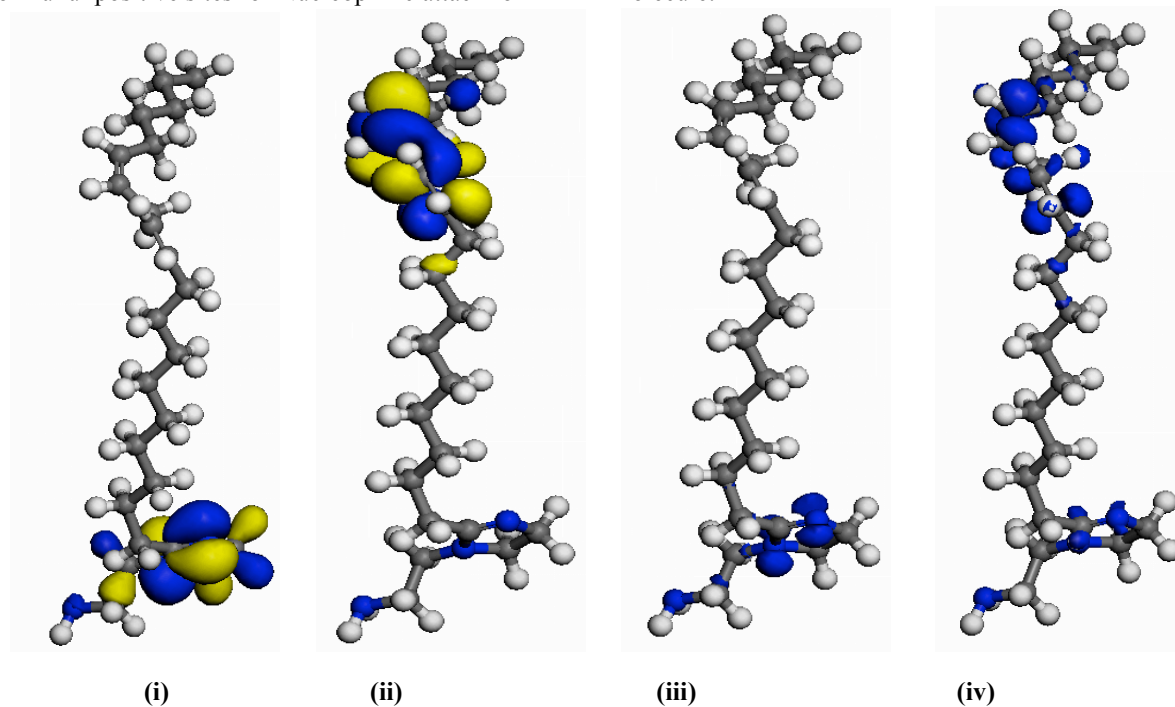


**Figure 4:** (i) HOMO orbital plot (ii) LUMO orbital plot (iii) Plot for Fukui negative sites for electrophilic attack (iv) Plot for Fukui positive sites for Nucleophilic attack for NDDE molecule.

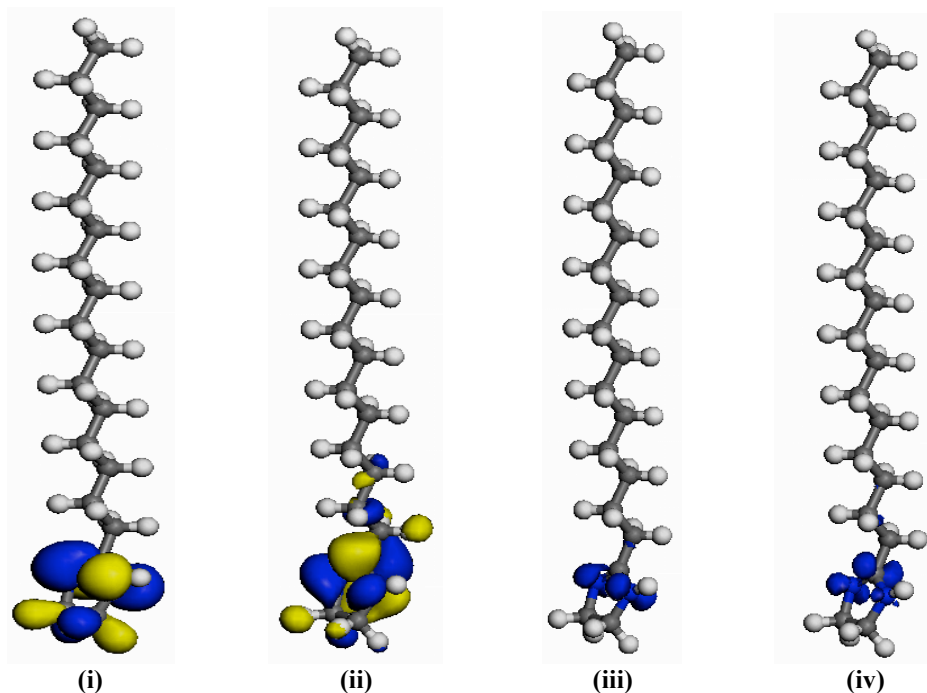


**Figure :5** (i) HOMO orbital plot (ii) LUMO orbital plot (iii) Plot for Fukui negative sites for electrophilic attack (iv) Plot for Fukui Positive sites for nucleophilic attack for HDDE molecule.

### 3.4. Molecular dynamic simulation

To obtain more information on the adsorption behavior of HDED, NDDE and HDDE, molecular dynamic simulation study was performed to simulate the adsorption of HDED, NDDE and HDDE on Fe (001) surface, and to further analyze the interactions between the three (3) molecules on the iron surface. The molecules are placed separately in each of the iron surface and the simulation module was run. The close contacts between the molecules and the iron surface as well as the best possible adsorption configurations for the molecules are shown in Figure 6.

The calculated interaction and binding energies obtained from the molecular dynamics simulations are presented in Table 5. The lowest interaction energies were considered for each of the possible modes of adsorption. The higher negative values of interaction energy can be attributed to the strong adsorption between the molecules and the iron surface [38] leading to better adsorption/corrosion inhibitive effect. From Table 5, the calculated values for the interaction energies during the simulation process shows that NDDE has the lowest value of the interaction energy followed by HDED, while HDDE having the highest value of the interaction energy. Therefore, the decreasing order for adsorption/corrosion inhibitive potential of the studied molecules are NDDE > HDED > HDDE. Furthermore, the higher magnitude of binding energy for NDDI, presented in Table 5 also suggests a more stable adsorption system for NDDI with higher adsorption/corrosion inhibitive potential [39]. The stability of the molecules and their adsorption/corrosion inhibitive potential are ranked in decreasing order as NDDE > HDED > HDDE. These results are in good agreement with the results obtained from the theoretical quantum chemical calculations. From Figure 6, the molecules are seen attached to the iron surface using the heterocyclic ring and pendent part where the HOMO orbital densities are found, due to the fact that the values of  $\Delta N$  for these molecules are lesser than 3.6 which suggests that the adsorption will be solely due to the electron donating ability of these molecules. This also confirms the statement made in the quantum chemical calculation section, that the part of the molecule with high HOMO density will be oriented towards the iron surface. The exposed iron surface can be made corrosion resistant by the covering of the surface brought about by the strong attachment of NDDE, HDED and HDDE molecules on the iron surface, and also the covering made by the alkyl hydrophobic tail possessed by these molecules from the agents of corrosion.

**Table 5:** Interaction and binding energies between the molecules and the Fe (001) surface.

Systems	$E_{\text{interaction}}$ (Kcal/mol)	$E_{\text{binding}}$ (Kcal/mol)
Fe (001) + HDED	-109	109
Fe (001) + NDDE	-113	113
Fe (001) + HDDE	-73	73

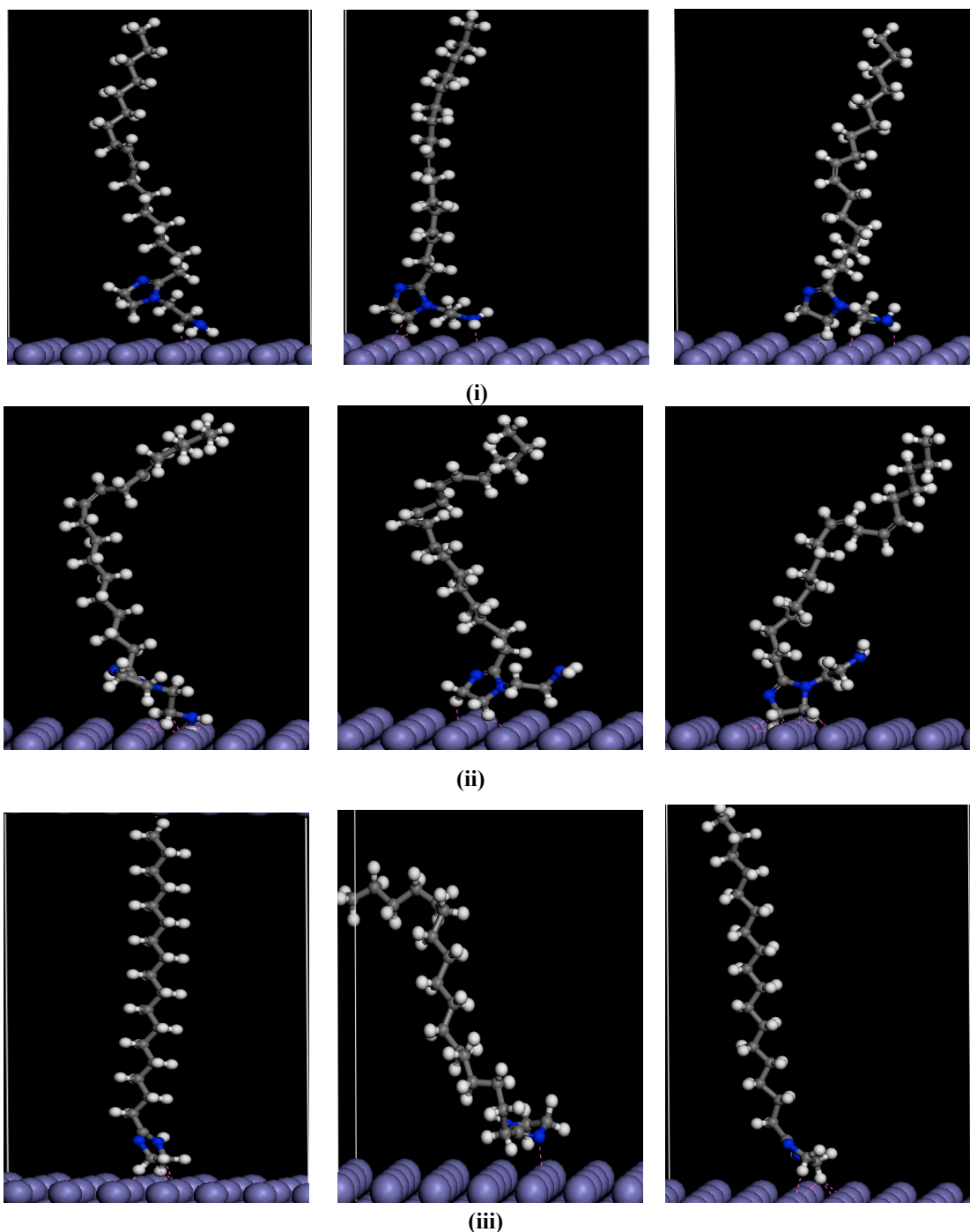


**Figure 6:** Best possible adsorption configurations for (i) HDDE, (ii) NDDE and (iii) HDDE molecules on Fe (001) surface.

### Conclusion

From the results and findings of the study, the quantum chemical calculations revealed the active sites for adsorption on these molecules based on the natural atomic charge, the frontier molecular orbitals, the Fukui indices and plots, bond length and bond order analysis to be the nitrogen and some carbon atoms present in the molecules. with the major sites for adsorption by which the molecules can directly adsorb onto the iron surface mainly by donating electron to the iron atoms to be the N7=C8-N4 region in the heterocyclic ring for HDDE and NDDE molecules, and the N4=C5-N1 region in the heterocyclic ring for HDDE molecule. The molecular dynamic simulation suggested that the three (3) molecules are physically adsorbed on the iron surface in a perpendicular manner using mainly the heterocyclic ring part of the molecules, with a high negative adsorption energy. The order of the adsorption/corrosion inhibitive potential for the quantum chemical calculations is in agreement with the order obtained from the molecular dynamic simulation and it is given in decreasing order as NDDE > HDDE > HDDE. The order of the adsorption/corrosion inhibitive potential of these molecules supports the findings of Umoren and Gasem, [40]; Okafor *et al* [41] which says that molecules with higher

molecular weight inhibit better than molecules with lower molecular weight. The molecules can be said to act as corrosion inhibitors. This work is a good example of how computational chemistry can be used as a screening tool to test several different molecules, and more importantly to develop an understanding on the behavior of different systems as a function of their molecular characteristics.

## References

1. M.G. Fontana, *Corrosion Engineering*, Mc Graw- Hill International, New York, (1987). P.4,
2. E. Khamis, N. Al- Andis, *Mater. Wissen. Werk.* 33 (2002) 550-554.
3. K.F. Khaled, *Electrochimica Acta.* 48 (2003) 2493-2501.
4. F. Touhami, A. Aounti, *Corros Sci.* 42 (2000) 929-940.
5. J.M. Bastidos, J. Damborenea, A.J. Vazquez, *J. Appl. Electrochem.* 27 (1997) 34-51.
6. I.B. Obot, N.O. Obi-Egbedi, *Surf Rev Lett.* 15 (2008) 903-910.
7. S.S. Abd El-Rehim, M.A. Ibrahim, F.F. Khaled, *J. Appl. Electrochem.* 29 (1999) 593-599.
8. E.E. Ebenso, D.A. Isabirye, N.O. Eddy, *Int. J. Mol. Sci.* 11 (2010) 2473-2498.
9. S. Xia, M. Qui, L. Yu, F. Lui, H. Zhao, *Corros Sci.* 50 (2008) 2012-2029.
10. S. Saha, A. Hens, A. RoyChowdhury, A. Lohar, N.C. Murmu, P. Banerjee, *Can Chem trans.* 2 (2014) 489-503.
11. A.Y. Musa, R.T. Jalgham, A. Mohamad, *Corros Sci.* 56 (2012) 176-183.
12. K.J. Uwakwe, A.I. Obike, *Int Res J Pure Appl Chem.* 15 (2017) 1-11.
13. K.F. Khaled, *Electrochimica Acta.* 53 (2008) 3484-3492.
14. P. Udhayakala, *J Chem Pharm Res.* 7 (2015) 803-810.
15. K.F. Khaled, *Electrochimica Acta.* 54 (2009) 4345-4350.
16. L.Tang, L. Yao, C. Kong, W. Yang, Y. Chen, *Corros Sci.* 53 (2011) 2046-2052.
17. A. Hassazadeh, *Electrochimica Acta.* 51 (2004) 305-316.
18. Material studio, version 5.0, Accelrys Inc, San Diego, USA, 2009.
19. J. Liu, W. Yu, J. Zhang, S. Hu, L. You, G. Qiao, *Appl. Surf. Sci.* 256 (2010) 4729-4733.
20. T. Koopmans T, *Physica.* (1933) 104-113.
21. R.G. Parr, R.G. Pearson, *J. Am. Chem. Soc.* (1983) 7512-7516.
22. S. Martinez, *Mater. Chem. Phys.* 77 (2003) 97-102.
23. P. Parida, B. Ganguli, A. Mookerjee, arXiv: 1410.3185v1 [cond-mat.mtrl-sci] 13 Oct 2014.
24. M.J.S. Dewar, W. Thiel, *J. Am. Chem. Soc.* 99 (1977) 4899-4907.
25. C. Wang, D. Chang, C. Tang, J. Su, Y. Zhang, Y. Jia, *J Mod Phys.* 2 (2011) 1067-1072
26. R.G. Parr, L. Szentpaly, S. Liu, *J. Am. Chem. Soc.* 121(1999) 1922.
27. W. Yang, W. Mortier, *J. Am. Chem. Soc.* (1986) 5708- 5713.
28. M.A. Quijano, M.P. Pardav, A. Cuan, M.R. Romo, G.N. Silva, R.A. Bustamante, A.R. Lopez, H.H. Hernandez, *Int. J. Electrochem. Sci.* 6 (2011) 3729-3742.
29. U. Maeder, R.N. Swamy, *Corrosion and Corrosion Protection of Steel in Concrete*, Sheffield Academic Press, Sheffield, UK, 1994, p. 851.
30. S.L. Li, Y.G. Wang, S.H. Chen, R. Yu, S.B. Lei, H.Y. Ma, D.X. Liu, *Corros Sci.* 41 (1999) 1769-1782.
31. A. Yurt, S. Ulutasa, H. Dal, *Appl. Surf. Sci.* 253 (2006) 919-925.
32. K.F. Khaled, M.A. Amin, N.A. Al-Mobarak, *J. Appl. Electrochem.* 40 (2010) 601-613.
33. M. Fay, *Chemistry 4<sup>th</sup> Ed*, Pearson Education, New Jersey, (2004).
34. V.F. Ekpo, P. C. Okafor, U.J. Ekpe, E.E. Ebenso, *Int. J. Electrochem. Sci.* 6 (2011) 1045-1057.
35. I.B. Obot, N.O. Obi-Egbedi, E.E. Ebenso, A.S. Afolabi, E.E. Oguzie, *Res. Chem. Intermed.* 39 (2013) 1927-1948.
36. N.O. Obi-Egbedi, I.B. Obot, M.I. El-Khaiary, S.A. Umoren, E.E. Ebenso, *Int. J. Electrochem. Sci.* 6 (2011) 5649-5675.
37. I. Lukovits, E. Kalman, F. Zucchi, *Corrosion.* 57 (2001) 3-8.
38. A.Y. Musa, A.A.H. Kadhum, A.B. Mohamad, M.S. Takriff, *Corros. Sci.* 52 (2010) 3331-3340.
39. K.F. Khaled, *J. Appl. Electrochem.* 41 (2011) 423-433.
40. S. Umoren, Z. Gasem, *J Disper Sci Technol.* 35 (2013) 1181-1190.
41. P.C. Okafor, E.E. Ebenso, U.J. Ekpe, *Bull Chem Soc Ethiop.* 18 (2004) 181-192.

(2018) ; <http://www.jmaterenvirosci.com>